

**2236-Plat****Analysis of the Cellulose-Cellulase Interaction**Emal M. Alekozai<sup>1</sup>, Xiaolin Cheng<sup>2</sup>, Jeremy C. Smith<sup>3</sup>.<sup>1</sup>Interdisciplinary Center for Scientific Computing, University of Heidelberg, Heidelberg, Germany, <sup>2</sup>ORNL Center for Molecular Biophysics, Oak Ridge National Laboratory, Oak Ridge, TN, USA, <sup>3</sup>ORNL Center of Molecular Biophysics, Oak Ridge National Laboratory, Oak Ridge, TN, USA.

Cellulose holds great potential as a source of biofuel energy. It is a complex carbohydrate that forms the cell walls of plants and gives them rigidity. The sugar subunits can be unlocked and fermented to produce ethanol. Plants have developed over time defense mechanism which locks up sugars and makes the fermentation process difficult and not cost-competitive [1]. The cellulase enzyme CBH1 [2] is capable to break up this sugar chains, it consists of two parts, the binding module and the catalytic domain which are hold together by a linker peptide. One of the major research questions is to analyze the mechanical process how the cellulase enzyme accesses the cellulose fiber. There is evidence that the linker peptide shows a high flexibility and could be essential for the understanding of the cellulase dynamic.

To guarantee statistical unbiased results a set of Brownian dynamics simulations are performed. The huge configuration space is discretized by applying different clustering algorithms. A Markov state model (MSM) [3,4] was used to analyze the dynamics of the system. The MSM description gives a mathematically rigorous approach to combine the statistical information of several independent simulations. There is no clear experimental evidence in which order the different enzyme parts access the fiber. In the context of a MSM the probability for different docking conformations of the fiber are calculated to answer this question. Depending on the bundling schema of the cellulose fibers, different phases are visible. It is further analyzed if the enzyme favors one of the fiber phases to split up the sugar chains.

[1] Himmel et al, Science, 2007

[2] Brady et al, Cellulose, 2008

[3] Bremaud, Springer, 1999

[4] Singhal et al, JPC, 2004

**2237-Plat****Single Molecule Kv2.1 Channel Dynamics in Live Mammalian Cells**

Aubrey V. Weigel, Michael M. Tamkun, Diego Krapf.

Colorado State University, Fort Collins, CO, USA.

Neuronal Kv2.1 potassium channels localize into micron-sized clusters which are regulated by extracellular glutamate and intracellular Ca<sup>2+</sup> levels. The physical mechanisms underlying the formation and maintenance of these unique structures are largely unknown. We are investigating the dynamics of clustered Kv2.1 channels using high resolution total internal reflection fluorescence microscopy (TIRFM) to track single molecules with 8 nm accuracy.

Transfected human embryonic kidney (HEK) cells expressing biotinylated and GFP-tagged Kv2.1 channels are detected with streptavidin-conjugated red quantum dots (QD). While the red QDs enable tracking of individual channels, GFP fluorescence provides characteristics of clusters as an ensemble. The channel dynamics inside Kv2.1 clusters are analyzed in the membrane of live cells in terms of their mean square displacement (MSD) and cumulative distribution function (CDF).

In our current model, the actin cytoskeleton plays a dominant role in Kv2.1 cluster formation and maintenance. To test this model we are studying the effects of depolymerization agents such as Cytochalasin and Swinholid A on the individual channel dynamics.

Clustered channels remain confined within the cluster perimeter throughout the entire imaging time, up to 25 minutes. MSD analysis indicates similar diffusion constants for clustered and non-clustered channels,  $D = 0.013 \pm 0.017 \mu\text{m}^2/\text{s}$  and  $0.014 \pm 0.011 \mu\text{m}^2/\text{s}$  respectively. The CDF of all analyzed trajectories ( $n=900$ ) deviates from a monoexponential, indicating a discrepancy with Brownian diffusion. Instead, the data can be accurately fit to a double exponential. Our results show a bimodal distribution of channels (clustered and non-clustered) and indicate that both populations experience anomalous subdiffusion. The double exponential term of the CDF suggests two stochastic processes which have slow and fast mobility respectively. Single molecule tracking with simultaneous channel cluster imaging is shown to be an effective way to study the mechanisms underlying clustering phenomena.

**2238-Plat****Illuminating Dynamic Regions Associated with the Heterotropic Allosteric Communication In Bacillus Stearothermophilus Phosphofructokinase**

Stephanie A. Perez, Gregory D. Reinhart.

Texas A&amp;M Univ, College Station, TX, USA.

Van't Hoff analysis has revealed that the positive sign of the coupling free energy between the allosteric inhibitor, phosphoenolpyruvate (PEP), and the sub-

strate, fructose 6-phosphate (F6P), of *Bacillus stearothermophilus* phosphofructokinase (BsPfk) is determined by the large entropy component of the system. BsPfk can exist in four different ligation states: BsPfk-F6P, PEP-BsPfk, PEP-BsPfk-F6P, and apo-BsPfk. The coupling free energy derives from the standard free energy associated with the equilibrium between the first 2 and the last 2 species, respectively. However the entropic properties of these species are poorly understood. The dynamic character of these four species can be expected to contribute to the coupling entropy which we have investigated using intrinsic tryptophan fluorescence anisotropy to report on the local restrictions to side-chain motion. Hybrid forms of BsPfk containing a single tryptophan that report on a single heterotropic interaction have been constructed. Tryptophan was positioned by constructing conservative tryptophan-shift modifications in which one of the sixteen native phenylalanine or tyrosine residues in one subunit was substituted with tryptophan, and the native tryptophan was changed to a tyrosine. Six positions dispersed throughout the monomer were initially targeted for this modification. Steady-state anisotropy measurements combined with time-resolved experiments were used to detect significant changes in the rotational correlation times of each ligated species of the BsPfk hybrid that isolates the strongest single heterotropic interaction. The dynamic changes observed in this manner suggest that specific regions are involved in the heterotropic allosteric coupling. Of the dynamics measured between the enzyme forms relevant to the coupling, F139 and F240 exhibit the largest difference in dynamics suggesting these residues identify regions particularly important for the allosteric communication of the dominant heterotropic interaction in BsPfk. Supported by NIH Grant GM33216 and Welch Foundation Grant A1548.

**2239-Plat****Proteins of Functioning Flagellar Rotor Turnover but only in the Presence of Signalling Proteins**

Nicolas J. Delalez, George H. Wadhams, Richard M. Berry,

Judith P. Armitage, Mark C. Leake.

University of Oxford, Oxford, United Kingdom.

For many bacteria, motility is achieved by means of one or more filaments, each being driven by a rotary motor embedded in the cell membrane. The bacterial flagellar rotary motor is one of nature's most intricate molecular machines and is composed of two main parts: the rotor and the stator. Whilst much is known about its static structure, there are little data on the dynamics and interactions of its constituents under natural conditions in living cells. Recent results revealed the rapid exchange undergone by the membrane spanning protein complex MotAB which localizes around the rotor and forms the torque generating units. The C-ring, also called "switch complex", is part of the rotor and is localized to the cytoplasmic region of the motor. The response regulator CheY-P binds one of the C-ring components, FliM, causing the rotor to switch rotational direction thus making FliM the interface with the chemosensory pathway.

Here, we use single-molecule fluorescence imaging in *Escherichia coli* cells expressing genomically-encoded YPet derivatives of FliM at physiological levels. Analysis of functional flagellar motors revealed that each contains ~34 FliM molecules. We found that two FliM populations coexist within the same motor, one undergoing constant turnover and one remaining "fixed". Surprisingly, exchange within the dynamic population relies on the presence of the response regulator protein linking the complex to the rest of the sensory pathway and may therefore play an active part of signal processing within the cell.

These results show the strength of combining molecular genetics with *in vivo* imaging and in this case illustrate the highly dynamic and adaptive nature of the bacterial flagellar motor. Further data will be presented on the different FliM complexes observed in the cells and their possible interaction with CheY-P.

**Platform AP: Membrane Pumps & Transporters****2240-Plat****Single Molecule Rotation of F1-ATPase from *S. cerevisiae***Bradley C. Steel<sup>1</sup>, Yamin Wang<sup>2</sup>, Vijay Pagadala<sup>2</sup>, Richard M. Berry<sup>1</sup>,David M. Mueller<sup>2</sup>.<sup>1</sup>University of Oxford, Oxford, United Kingdom, <sup>2</sup>Rosalind Franklin

University of Medicine and Science, North Chicago, IL, USA.

Single molecule studies of the thermophilic *Bacillus* PS3 F<sub>1</sub>-ATPase have revealed kinetic and structural information that cannot be discerned using other methods, including the presence of 40 and 80 degree physical substeps (Yasuda *et al.* 2001) and the order and kinetics of chemical substeps. We use single molecule techniques to observe the effects of Mitochondrial Genome Integrity

mutations on enzyme kinetics and torque production in  $F_1$  from the yeast *S. cerevisiae*.

Mitochondrial Genome Integrity (*mg1*) mutations allow yeast to survive the loss of mitochondrial DNA. A number of these mutations occur in the genes encoding the  $F_1$  portion of the ATP Synthase, and have been shown to uncouple ATP Synthase (Wang *et al.* 2007). The mutations cluster around the collar region of  $F_1$  where the alpha, beta and gamma subunits interact and are thus likely to affect  $F_1$  rotation.

Using a high speed camera and a novel method for laser darkfield microscopy, we captured the rotation of wild-type and *mg1* forms of yeast  $F_1$ -ATPase. We show for the first time that at saturating ATP, wild-type yeast  $F_1$  rotates approximately four times faster than the thermophilic  $F_1$ . Kinetic and substepping behaviour in wildtype yeast appears to be similar to that observed in bacterial  $F_1$ , but some of the *mg1* forms show behaviour that is different to both wildtype and previously reported forms of  $F_1$ . We will use the results from these single molecule experiments in conjunction with structural studies to elucidate the mechanisms underlying rotation in wildtype and *mg1* forms of  $F_1$ .

This work was supported by NIH R01GM066223.

#### 2241-Plat

##### Mechanisms of Selective Sodium/proton Binding and Coupled Rotation in F1fo ATP Synthases: Insights from Quantitative Computer Simulations

Alexander Krah, Peter J. Bond, José D. Faraldo-Gómez.

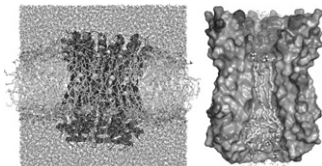
Max Planck Institute of Biophysics, Frankfurt am Main, Germany.

F-ATP synthases are the most prominent ATP source across the living world. These enzymes couple the structural changes required for catalyzing the conversion of ADP and  $P_i$  into ATP to the transmembrane flow of protons or sodium ions down their electrochemical gradients. The key, coupling element in these molecular machines is the membrane-embedded  $F_o$  rotor, or c-ring. The recent emergence of high-resolution structural data and the close interplay of experimental methods with advanced, quantitative molecular simulations are providing novel and important insights into the mechanisms of these essential proteins. We present an overall summary of our recent progress in this area, particularly pertaining to the mechanism by which ion exchange across the lipid membrane is coupled to the rotation of the c-ring, as well as to the structural basis for the distinct ion-binding selectivity observed for different species. We believe these principles may well apply more generally in the context of ion-coupled membrane transport.

Meier [...] Faraldo-Gómez (2009). *J. Mol. Biol.* 391:498-507.

Pogoryelov [...] Faraldo-Gómez, Meier. (2009). *Nat. Struct. Mol. Biol.* (in press).

Krah [...] Meier, Faraldo-Gómez (2009). *J. Mol. Biol.* (under review).



#### 2242-Plat

##### Mechanism of Selective Cation Binding to Sodium-Coupled Transporters: Insights from Free Energy Simulations and QM/MM Simulations

Sergei Noskov, Chunfeng Zhao, Lev Bogdan.

University of Calgary, Calgary, AB, Canada.

Ion-coupled transport of neurotransmitter molecules by secondary amino-acids transporters plays pivotal role in the regulation of neuronal signaling. One of the major events in the transport cycle is ion-substrate coupling and formation of the high-affinity occluded state with bound ions and substrate. Molecular mechanisms of ion-substrate coupling, specificity for a particular cation and the corresponding ion-substrate stoichiometry in secondary transporters has yet to be understood. We have studied  $Li^+/K^+/Ti^+/Na^+$  binding and/or selectivity to several transporters with available crystal structures such as the bacterial aspartate transporter GltPh, leucine transporter LeuT and maltose transporter vSGLT using free energy simulations and QM/MM minimization to evaluate the role of different factors in the observed selectivity and ion binding to the protein. Two different mechanisms were found to co-exist for crystallographically characterized binding sites Na1 and Na2 in LeuT and Glt. Furthermore, site Na1 appeared to be well conserved amongst members of different families. To evaluate the role of  $Na^+$  binding in the transporter function, we have performed free energy simulations to determine actual cation selectivity as well as binding affinity for sites Na1 and Na2 in the protein. QM/MM minimization was used to characterize the role of the electronic effects of the stabilization of non-native cations such as  $Li^+$  and  $Ti^+$  in the  $Na^+$ -selective sites of different transporters. In the case of  $Ti^+$  binding to Glt transporter, neighboring residues from a second solvation shell provide a necessary stabilization to

the larger cation due to polarization and charge transfer effects implying a rather large flexibility of the metal binding sites.

#### 2243-Plat

##### Computational Approaches to Understanding the Mechanism of Transport in the $Na^+$ /galactose Co-Transporter vSGLT

Seungho Choe<sup>1</sup>, John Rosenberg<sup>1</sup>, Ernest Wright<sup>2</sup>, Jeff Abramson<sup>2</sup>, Michael Grabe<sup>1</sup>.

<sup>1</sup>Univ. of Pittsburgh, Pittsburgh, PA, USA, <sup>2</sup>UCLA, Los Angeles, CA, USA.

A number of recent high resolution structures suggest that a larger family of cation coupled substrate transporters share a common core architecture. At the molecular level, it is not known how this architecture enables them to harness the energy stored in ionic gradients to move small molecules across the membrane. We have studied the details of substrate and ion entry and exit to the cytoplasm of the galactose symporter vSGLT. We used equilibrium molecular dynamics (MD) simulations to determine the role of key residues in stabilizing galactose and sodium in their respective binding sites. The simulations show that the transporter is stable when simulated as a monomer having only small deviations from the x-ray structure. We also used steered MD simulations to pull galactose and sodium from their site into the cytoplasm to obtain the free energy for unbinding.

#### 2244-Plat

##### A Mutation Associated with DCM Increases Phospholamban Oligomerization and Decreases SERCA-Binding, but Does Not Change Phospholamban Tertiary Structure or Phosphorylation by PKA

Zhanjia Hou<sup>1</sup>, Raffaello Verardi<sup>2</sup>, Larry R. Masterson<sup>2</sup>, Naomi Menards<sup>2</sup>,

Kim N. Ha<sup>2</sup>, Alessandro Mascioni<sup>2</sup>, Gianluigi Veglia<sup>3</sup>,

Seth L. Robia<sup>1</sup>.

<sup>1</sup>Loyola University Chicago, Maywood, IL, USA, <sup>2</sup>University of Minnesota,

Minneapolis, MN, USA, <sup>3</sup>University of Minnesota, Minneapolis, MN, USA.

To better understand the pathological mechanism of a human dilated cardiomyopathy phospholamban (PLB) mutation (R9C), we investigated the effects of this mutation on PLB structure and regulatory interactions. Notably, we observed efficient phosphorylation of R9C-PLB by PKA *in vitro*, and nuclear magnetic resonance (NMR) spectroscopy showed no change in R9C-PLB structure compared to WT. To test R9C-PLB binding interactions in live cells, PLB was expressed as cyan and yellow fluorescent protein (CFP/YFP) fusions in AAV-293 cells, and PLB oligomerization and SERCA-binding were quantified by fluorescence resonance energy transfer (FRET). 100 micromolar  $H_2O_2$  applied to the cells induced a rapid quench of CFP-R9C-PLB fluorescence and a concomitant increase in YFP-R9C-PLB fluorescence, indicating an increase in intraoligomeric FRET after oxidation. FRET enhancement after peroxide addition was not observed for CFP/YFP-WT-PLB. To test whether the FRET increase was due to increased oligomerization or a quaternary conformation change, we measured intraoligomeric FRET in a population of cells expressing a wide range of R9C-PLB protein concentrations. FRET dependence on concentration yielded oligomer intrinsic FRET efficiency ( $FRET_{max}$ ) and relative dissociation constant ( $K_D$ ). Compared to WT, R9C-PLB had a decreased  $K_D$  and increased  $FRET_{max}$ , indicating an increased oligomerization affinity and more compact oligomer structure, respectively. The enhanced oligomerization of R9C-PLB was matched by a decrease in SERCA-binding compared to WT. Overall the data suggest a new mechanism by which the R9C mutation may exert a pathological effect: decreased SERCA regulation and increased oligomerization, as consequences of increased sensitivity of R9C-PLB to oxidation.

#### 2245-Plat

##### The $Na,K$ -ATPase Beta1 and Beta2 Subunits Associate with Different Quality Control Pathways in the ER

Olga Vagin<sup>1,2</sup>, Elmira Tokhtaeva<sup>1,2</sup>, George Sachs<sup>1,2</sup>.

<sup>1</sup>UCLA, Los Angeles, CA, USA, <sup>2</sup>VAGLAHS, Los Angeles, CA, USA.

The catalytic  $Na,K$ -ATPase  $\alpha$ -subunit is not able to exit the ER or catalyze ion transport unless assembled with the  $\beta$ -subunit. However, requirements for the ER exit of the  $Na,K$ -ATPase  $\beta$ -subunit that plays an additional, ion-transport-independent, role in intercellular adhesion are not clear. The  $Na,K$ -ATPase  $\beta_1$ - or  $\beta_2$ -subunits and their N-glycosylation-deficient mutants were expressed in renal MDCK cells. Confocal microscopy, immunohistochemistry, and immunoprecipitation were employed to evaluate the role of N-glycans of the  $\beta$ -subunit isoforms in the quality control of the  $Na,K$ -ATPase in the ER. Mutagenic removal of as few as two of the eight N-glycosylation sites from the  $\beta_2$ -subunit precludes its assembly with the  $\alpha_1$  subunit and results in full retention of the unassembled  $\beta_2$ -subunit in the ER. However, removal of all three N-glycosylation sites from the  $\beta_1$ -subunit only slightly affects its